Coacervation of Elastin-Like Recombinamer Microgels

Smriti Singh, Dan Eugen Demco,* Khosrow Rahimi, Radu Fechete, José Carlos Rodriguez-Cabello, Martin Möller*

The investigation of the coacervation (self-aggregation) behavior of biomicrogels which can potentially be used as drug carriers is an important topic, because self-aggregation can not only cause loss of activity, but also toxicity and immunogenicity. To study this effect microgels from elastin-like recombinamer are synthesized using miniemulsion technique. The existence of coacervation for such microgels, at different concentrations and temperatures, is studied and proved by cryo-field emission scanning clectron microscopy (cryo-FESEM), cryo-transmission electron microscopy (cryo-TEM), and by a novel ^{1}H high-resolution magic angle sample spinning (HRMAS), nuclear magnetic resonance (NMR) spectroscopy, and relaxometry methods. The findings by ^{1}H HRMAS NMR spectroscopy and relaxometry show simultaneous processes of volume phase temperature transition and coacervation with different sensitivity for hydrophobic and hydrophilic amino acid side-chains in the microgel. The coacervation process is more evidential by the behavior of glycine α-CH_2, ^{1}H NMR peak as compared to the proline β-CH_2.

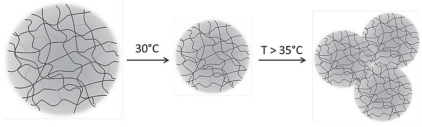

1. Introduction

In general, the selfassembly of colloids is an attractive avenue for the fabrication of nanostructured materials with interesting electrical, magnetic, and mechanical as well as responsiveness.[1] In the last years biohybrid microgels have been intensively investigated mainly due to the incorporation of specific functionality originating from the biological building blocks in the synthetic microgels.[2] Many of such bioobjects especially those based on polypeptide networks have the ability to undergo a volume phase transition in response to external stimuli, such as temperature, pH, and ionic strength. These characteristics of such microgels makes them attractive candidate for applications in the field of drug delivery.[3,4]

Recently, thermoresponsive and pH-responsive microgels were prepared from solubilized α-elastin derived from bovine neck ligament, by crosslinking of the lysine residues in elastin using the hydrophilic amine-reactive crosslinker poly(ethylene glycol) diglycidyl ether (PEGDGE).[5] For this biohybrid microgel, information about morphological and polypeptide–water interactions in the process of volume phase temperature transition (VPTT) were obtained by dynamic light scattering (DLS) at low concentration, ^{1}H high-resolution magic-angle sample spinning (HRMAS), nuclear magnetic resonance (NMR) spectroscopy, and relaxometry.[6] These microgels showed a reversible phase transition for the studied five cycles of heating and cooling.

Dr. S. Singh, Prof. D. E. Demco, Dr. K. Rahimi, Prof. M. Möller
DWI-Leibniz-Institute for Interactive Materials, e.V.
RWTH-Aachen University
Forckenbeckstraße 50, D-52074 Aachen, Germany
E-mail: demco@dwi.rwth-aachen.de; moeller@dwi.rwth-aachen.de
Prof. D. E. Demco, Prof. R. Fechete
Department of Physics and Chemistry
Technical University of Cluj-Napoca
25 G. Baritiu Str., RO-400027 Cluj-Napoca, Romania
Prof. J. C. Rodriguez-Cabello
G. I. R. Bioforge
University of Valladolid
CIBER-BBN, Valladolid 47011, Spain

Macromol. Rapid Commun. **2016**, *37*, 181–186

DOI: 10.1002/marc.201500457

Protein selfassembling is widely investigated mainly because of its connection to neurodegenerative diseases,[7,8] in the industrial processes for the production of therapeutic proteins as well as for estimation of shelf lifetime of medicaments.[9] Such type of selfassembling or coacervation is also present in recombinantly expressed human elastin polypeptides, as well as polypentapeptides and was shown to be mainly due to interactions between the hydrophobic domains.[10–14] Besides, the coacervation investigation of polypeptide biopolymers, the study of the selfassembly of thermally responsive nanoparticles synthesized from genetically encoded peptide polymer for drug conjugation was also reported.[15,16] A novel class of elastin like double-hydrophobic block polypeptides comprising proline-rich and glycine-rich segments have been reported showing coacervation of thermoresponsive nanofibers.[17] But there are very few studies on such coacervation behavior of biohybrid microgel, such studies are very important and relevant if such microgels are inclined to be used for drug delivery application.

The investigation of the coacervation behavior for the biohybrid microgels is an important topic because self-aggregation can cause loss of activity of biomolecules, as well as toxicity and immunogenicity. Hence, because of their toxic potential, aggregates can lead to an unwanted response or even overreaction of a patient's immune system. Thus to understand such behavior, in this study we use elastin-like recombinamer (ELR) microgels as a model. To the best of our knowledge no such investigation of the coacervation process of ELR microgels has been discussed so far.

The aim of this work is to use electron micrography and HRMAS NMR spectroscopy methods to show the existence of coacervation process, which can further be extended for other type of responsive microgel systems. The main advantage of the ^{1}H HRMAS technique is related to the possibility to access information about the behavior of hydrophobic and hydrophilic amino acids side chains that are revealed by ^{1}H high-resolution spectra.

2. Results and Discussion

2.1. Coacervation of ELR Microgels by Cryo-Field Emission Scanning Electron Microscopy (Cryo-FESEM) and Cryo-Transmission Electron Microscopy (Cryo-TEM) Micrographs

A visible proof of the ELR microgel coacervation was obtained form cryo-FESEM analysis. From the FESEM images it could be clearly seen that at low (2 mg mL^{-1}) and high (10 mg mL^{-1}) (Figure 1a,b) concentrations of the microgels at room temperature have a defined spherical shape and are monodispersed. While after heating at 55 °C for 5 h the sample of ELR microgels start to coacervate (Figure 1c,d). Considering a single microgel as a unimer, the coacervation behaviour is mainly dimeric to trimeric.

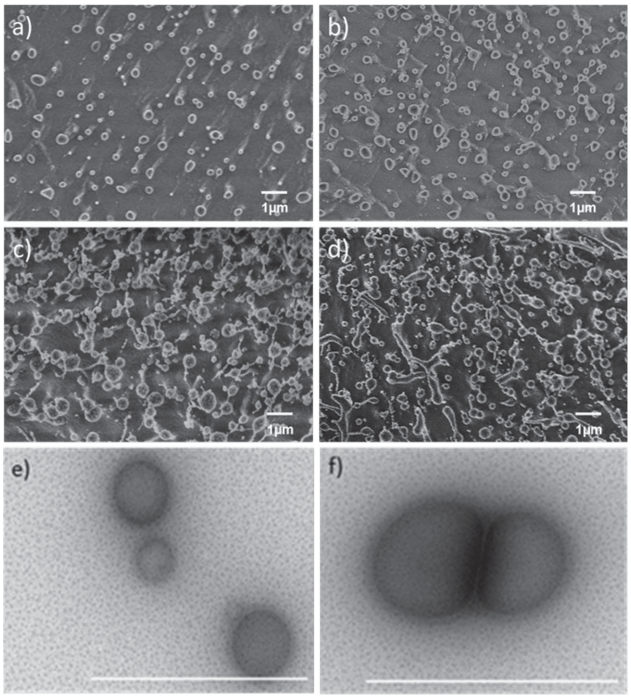

Figure 1. Cryo-FESEM images of ELR microgels: a) microgel concentration 2 mg mL^{-1} at room temperature, scale 1 μm, b) microgel concentration 10 mg mL^{-1} at room temperature, scale 1 μm, c) microgel concentration 2 mg mL^{-1} at room temperature after 5h heating at 55 °C, scale 1 μm, and d) microgel concentration 10 mg mL^{-1} at room temperature after 5h heating at 55 °C, scale 1 μm. Cryo-TEM pictures of ELR microgels with concentration of 8 mg mL^{-1} after incubation for 5 h at 55 °C. The coacervation of unimers in dimers for the incipient stage of the process is shown in e), scale 1 μm, and the fused dimers is shown in f), scale 1 μm.

The two stages of the coacervation process for ELR microgels are shown in Figure 1e,f. These micrographs were obtained by cryo-TEM using a sample with concentration of 8 mg mL^{-1} incubated at 55 °C for 5 h. The incipient stages of coacervation are shown in Figure 1e and the formation of a fused dimer in Figure 1f.

2.2. Proton HRMAS NMR Spectra of Native and ELR Microgels

To understand this process better, ^{1}H HRMAS NMR spectroscopy combined with relaxometry was performed and the results of the ELR microgels were compared to microgels derived from native α-elastin. A high-resolution NMR spectrum gives an access to the hydrophilic and hydrophobic amino-acid peaks in the microgels, due to fast rotation diffusion of the particles. This is possible due to averaging the dipolar interactions combined with sample rotation at the

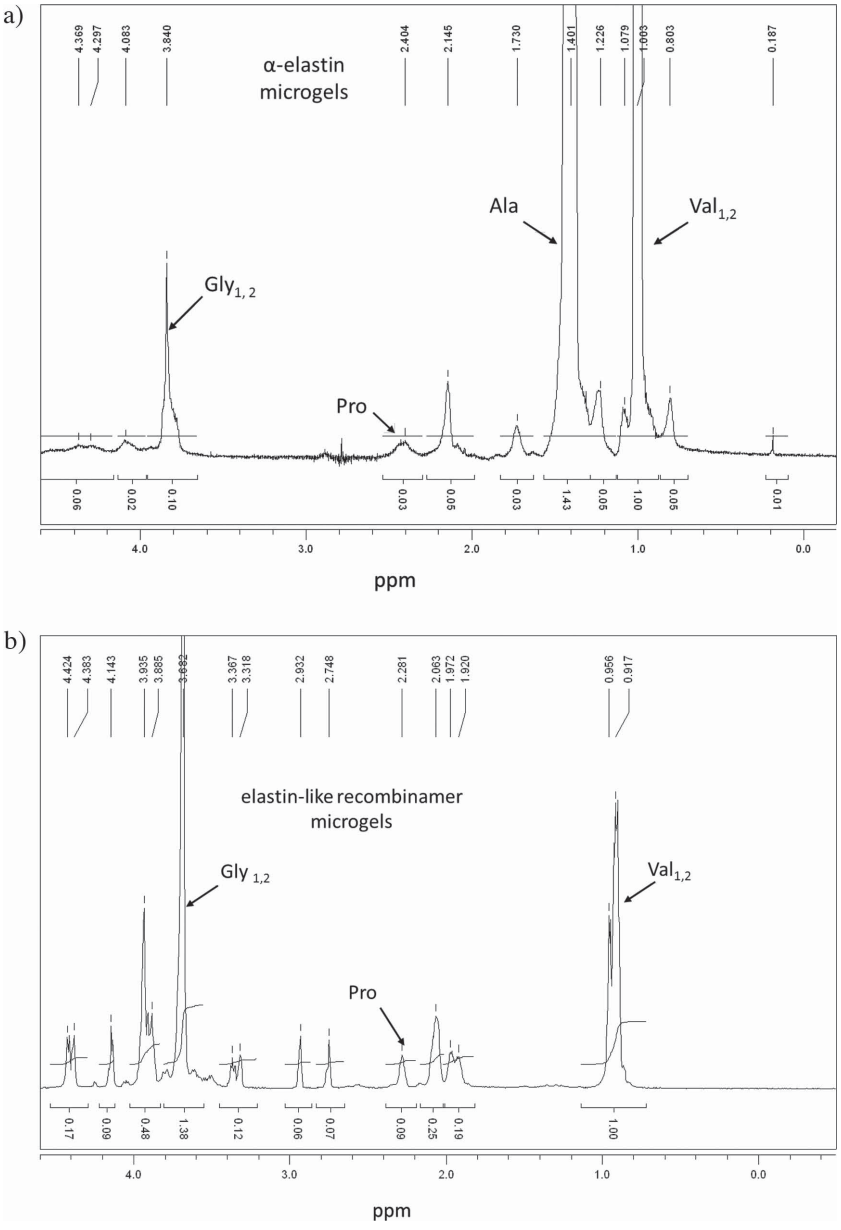

Figure 2. Aliphatic region of the ^{1}H HRMAS spectra at rotor frequency of 5 kHz and 23 °C of native α-elastin a) and ELR b) microgels with concentration of 2 mg mL^{-1} in D_2O. The polypetides were crosslinked with PEG-DGE having molar ratio of 1:1. The side-chains peaks of glycine (α-CH_2), proline (β-CH_2), alanine (β-CH_3) and valine (γ-CH_3) are marked by arrows.

magic angle. This spectral resolution is partially affected by the magnetic susceptibility mismatch between the microgels and solvent.

Proton HRMAS spectra in the aliphatic region of 0–4.6 ppm for the native, α-elastin and ELR microgels crosslinked by PEG-DGE with molar ratio of 1:1 at 23 °C are shown in Figure 2a,b. The peak assignment in the ^{1}H HRMAS spectra was made by a combination of ^{1}H spectra simulation of individual amino acids side chains in comparison to the ^{1}H spectra of two-synthetic elastin-like polypepentapeptides, poly(GVGVP) and poly(AVGVP) previously reported.[13] The ELR microgels were synthesized (see the Supporting Information) from the model recombinamer MGKKKP[$(VPGVG)_{14}$]$_6$, where the essential amino acids used for our investigation Val = L-valine, Gly = glycine, and Pro = L-proline are present.

^{1}H HRMAS spectra of α-elastin microgels reveals resolved peaks of hydrophobic valine (Val-γCH_3), alanine (Ala-βCH_2), and proline (Pro-βCH_2), (Figure 2a). The glycine (Gly-αCH_2) peak is partially superimposed on the alanine (Ala-αCH), proline (Pro-αCH), and PEG (CH_2) peaks. However, the signals in the aliphatic region of Gly_1 and Gly_2 as well as Val_1 and Val_2 cannot be resolved under MAS condition. But the well-organized structural domains of ELR microgels are reflected in sharp peaks of amino-acid side chains (Figure 2b). This is not the case for the native α-elastin microgels, where the structural heterogeneity leads to broad peaks especially into the glycine region (Figure 2a).

2.3. The Coacervation Process Revealed by Time-Dependent ^{1}H HRMAS NMR Spectroscopy

Proton NMR spectroscopy and relaxometry have difficulties to detect directly the coacervation kinetic for unimers, dimers, trimers, and *i*-mers. However, the presence of oligomers affects the transverse magnetization relaxation times (T_2) and leads to the peaks broadening and finally to a reduction in NMR integral spectral intensity. This is shown by the ELR microgels with 10 mg mL^{-1} concentration in D_2O (Figure S1, Supporting Information) incubated at different temperatures and times. The incubation time dependence of the ^{1}H HRMAS spectral integral intensities (Figure S1a, Supporting Information) shows that at 23 °C in the time interval of 200 min the coacervation process is very slow. While a clear thermal activation of the aggregation process is shown at 45 °C (Figure S1b, Supporting Information). The ^{1}H HRMAS NMR spectral intensity of the aliphatic region is decreasing with incubation time probing the coacervation process.

2.4. Combined Effect of Volume Phase Temperature Transition and Coacervation Process by ^{1}H HRMAS NMR T_2-Edited Spectral Integral Intensities of Amino-Acid Side-Chains

Recently, (DLS) that measures the hydrodynamic radius at low concentration of microgels was used to determine the VPTT of native, α-elastin microgel.[5,6] From the obtained data it was shown that the VPTT behaviour was reversible and the fact that the native α-elastin microgels remains soluble can be explained by the heterogeneous morphology of the microgels with a predominant corona formed by water-soluble segments of amino acids.[5]

It is known from the temperature sensitive synthetic microgels that, below the VPTT, they are in a swollen state, given by the dissolution of the hydrophilic groups in water through formation of hydrogen bonds.[18] Above this temperature, water is expelled from the microgel, and the hydrophobic groups are free to interact, which leads to phase separation and collapse of the microgels. The microscopic mechanism of VPTT for ELR microgels is different. The predominant way of hydration of the ELR microgels below their VPTT (T_t) is hydrophobic hydration. That is the formation of ordered water structures, surrounding the apolar moieties of the amino-acids side chains in the ELR microgels. It is the rupture of such water cages above T_t which enables the existence of hydrophobic contacts, collapse of microgel and also can induce coacervation. The most substantial percent of expelled water once above T_t is the hydrophobic hydration water. Similar behaviour was also observed for native α-elastin[6] but the phase change for ELR microgel after 5h above the VPTT is irreversible.

The swelling/deswelling process of microgels as well as selfassembly modifies the side chains mobility and interproton dipolar interactions due to the changes in the microgel/aggregate rotational diffusion, translational diffusion, and the local segmental motions of the biopolymer network. These are directly reflected in the values of transverse relaxation time T_2 and hence in the normalized integral intensities I/I_0 of the NMR peaks of the ^{1}H HRMAS spectra. In the case of VPTT process the temperature (T) dependence of the ratio I/I_0 can be described by the ad hoc sigmoidal or Boltzmann function[19]

$$\frac{I}{I_o}(T) = \frac{a}{1+\exp\left\{\frac{T-T_t}{\Delta T_t}\right\}} + b \quad (1)$$

where T_t is the transition temperature, ΔT_t describes the width of volume phase temperature transition, b is the plateau at large temperature and the a quantity is defined by $\frac{I}{I_o}(T_t) = \frac{a}{2} + b$. Furthermore, the fit of the experimental data with a Boltzmann function will lead us to the possibility to characterize quantitatively the heterogeneity of this continuous first order transition. This quantity is related to the chemical composition of microgels, cross-link density, the solvent, the interactions leading to

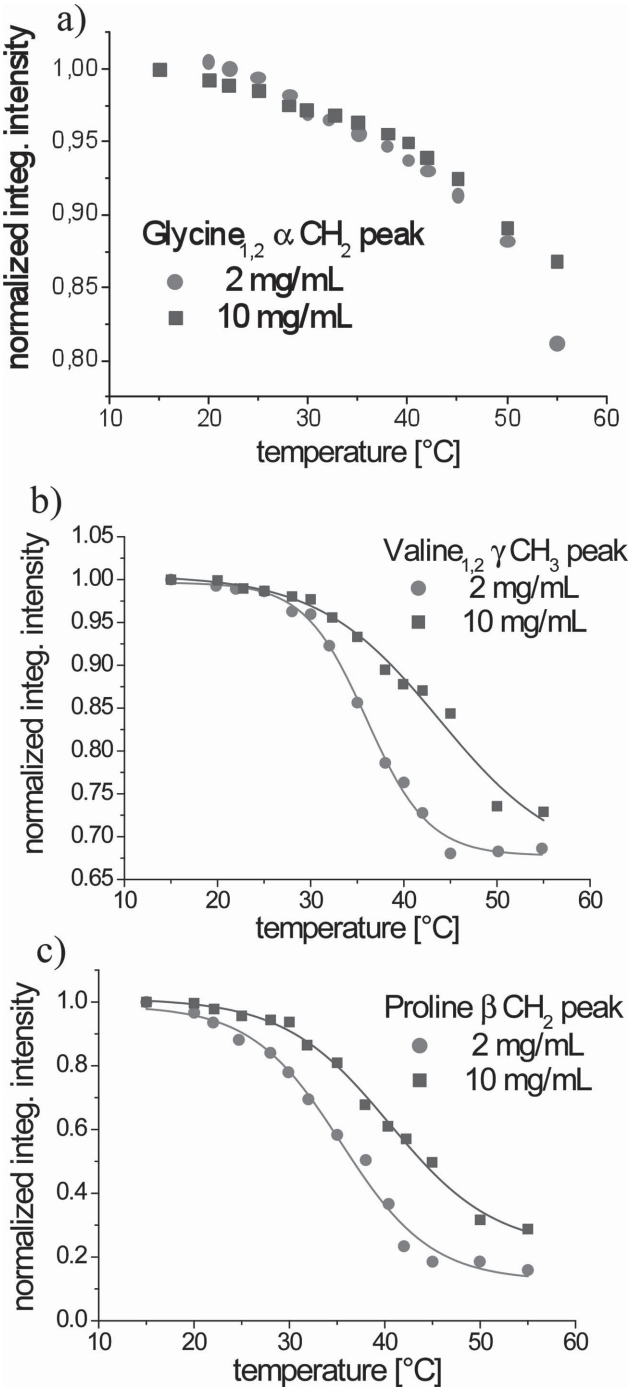

Figure 3. Volume phase temperature transition dependences in combination with coacervation measured from the ^{1}H HRMAS integral intensities of the glycine a), valine b), and proline c) for ELR microgels with concentration of 2 and 10 mg mL^{-1} in D_2O. The continuous lines are fits with the Boltzmann function (Equation (1)) and the fit parameters are reported in Table 1.

Table 1. The effective temperature ($T_{t,eff}$) and the effective width ($\Delta T_{t,eff}$) of the combined effect of volume phase temperature transition and coacervation of ELR microgel. These parameters are obtained by the fit of the data with the Boltzmann function Equation (1). The microgels used have 1:1 molar crosslink ratio of PEG-DGE at two concentrations in D_2O.

Amino acid	$T_{t,eff}$ [a)] [°C] 2 mg mL^{-1}	$\Delta T_{t,eff}$ [a)] [°C] 2 mg mL^{-1}	$T_{t,eff}$ [a)] [°C] 10 mg mL^{-1}	$\Delta T_{t,eff}$ [a)] [°C] 10 mg mL^{-1}
Proline	35.4	4.7	40.4	5.5
Valine	35.9	3.3	43.8	6.5

a)The fit errors are of the order of 10%.

the formation of aggregates, as well as the distribution and sizes of clusters.

The temperature dependences of the normalized spectral integral intensities in the aliphatic region measured for ELR microgel with concentration of 2 and 10 mg mL^{-1} using ^{1}H HRMAS T_2-edited spectra are shown in Figure 3. The valine and proline side chains show a sigmoidal shape revealing that the presence of coacervation will not dominate the VPTT process. Nevertheless, the temperature dependences of 2 and 10 mg mL^{-1} are different (Figure 3b,c) showing a larger coacervation effect induced by larger concentration at 10 mg mL^{-1}. This is fully supported by the self-diffusion measurements as shown in Figure S2 (Supporting Information). The sigmoidal curves are shifted to higher temperatures having a broader width as microgel concentration is increased. The effect of both processes is taken into account by an effective transition temperature $T_{t,eff}$ and transition width $\Delta T_{t,eff}$ obtained by the fit with Boltzmann function, Equation (1). The results are shown in Table 1. The presence of ELR microgel coacervation at 10 mg mL^{-1} is shown by the higher values of $T_{t,eff}$ compared to that for 2 mg mL^{-1} microgel (Table 1). The proline and valine side chains show larger temperature transition heterogeneity at 10 mg mL^{-1} reflected in the values of $\Delta T_{t,eff}$ that increases with microgel concentration (Table 1). That is a signature of coacervation having larger efficiency at higher concentration and temperature leading to the heterogeneity of volume phase transition. The existence of a coacervation process was also proved besides, the temperature dependence of the integral spectral intensity shown in Figure 3 by the measurements of self-diffusion coefficients (diffusivity D) as a function of microgel concentrations. For the same series of ELR microgels the dependence of diffusivity versus microgel concentrations is shown in Figure S2 (Supporting Information).

While a different behaviour is shown by glycine compared to proline and valine, which cannot be analysed by a Boltzmann function (Figure 3a). This could be partially related to the fact that glycine peak at 3.8 ppm is superimpose on the PEG methylene peak. The temperature dependence of the integral intensity is convex for all temperatures (Figure 3a). That shows that the coacervation process affects more the glycine side chains compared to that of proline. This is also valid for valine side chains at a concentration of 10 mg mL^{-1} (Figure 3b) which shows a distorted sigmoidal curve. This proves that the coacervation efficiency is dominated by the hydrophobic domains of ELR microgel. Furthermore, we can mention that the simultaneous presence of coacervation at different temperatures simultaneously with VPTT makes the analytical description of this combined process a complex task.

3. Conclusion

The coacervation of ELR microgels was revealed by cryo-FESEM, cryo-TEM micrographs and ^{1}H HRMAS, T_2-edited spectroscopy. The coacervation process of ELR microgel is taking place simultaneously with the VPTT. The sensitivity to the coacervation and volume phase transition is increased by using ^{1}H HRMAS spectra encoded by the transverse relaxation and edited by the spin echo. The amino-acid side chains show different ^{1}H HRMAS NMR sensitivity to the coacervation compared to the VPTT. This is due to the fact that the coacervation efficiency is dominated by the hydrophobic domains. Study of the ELR microgels coacervation and the conditions under which this process is taking place will allow the intelligent design of carriers in drug delivery systems.

Supporting Information

Supporting Information is available from the Wiley Online Library or from the author.

Acknowledgements: Financial support from DFG-SFB(A1) project is gratefully acknowledged. This project has received funding from the European Union's Horizon 2020 research and innovation programme under the Marie Sklodowska-Curie grant agreement No 642687: BIOGEL, the author J.C.R.-C. acknowledges financial support by the MINECO in projects MAT2013-41723-R and MAT2013-42473-R. The authors R.F. and D.E.D. gratefully acknowledge support by a grant of the Romanian National Authority for Scientific Research, CNCS-UEFISCDI, project number PN-II-ID-PCE-2011-3-0544 (PN II IDEI 307/2011).

Received: August 1, 2015; Revised: September 16, 2015; Published online: October 28, 2015; DOI: 10.1002/marc.201500457

Keywords: biohybrids; coacervation; elastins; electron micrography; ^{1}H NMR relaxometry; ^{1}H NMR spectroscopy; microgels; recombinant elastin

[1] L. Cademartiri, K. J. M. Bishop, *Nat. Mater.* **2015**, *14*, 2.
[2] S. Singh, M. Möller, A. Pich, *J. Polym. Sci. A Polym. Chem.* **2013**, *51*, 3044.
[3] J. K. Oh, R. Drumright, D. J. Siegwart, K. Matyjaszewski, *Prog. Polym. Sci.* **2008**, *33*, 448.
[4] A. V. Kabanov, S. V. Vinogradov, *Angew. Chem. Int. Ed.* **2009**, *48*, 5418.
[5] S. Singh, F. Topuz, K. Albrecht, J. Groll, M. Möller, *Adv. Polym. Sci.* **2013**, *12*, 268.
[6] A. Balaceanu, S. Singh, D. E. Demco, M. Möller, *Chem. Phys. Lett.* **2014**, *612*, 182.
[7] F. Chiti, P. Webster, N. Taddei, A. Clark, M. Stefani, G. Ramponi, C. M. Dobson, *Proc. Natl. Acad. Sci. USA* **1999**, *96*, 3590.
[8] P. Arosio, S. Rima, M. Lattuada, M. Morbidelli, *J. Chem. Phys. B* **2012**, *116*, 7066.
[9] W. Wang, *Int. J. Pharm.* **2005**, *289*, 1.
[10] D. W. Urry, *J. Protein Chem.* **1988**, *7*, 1.
[11] B. Vrhovski, S. Jensen, A. S. Weiss, *Eur. J. Biochem.* **1997**, *250*, 92.
[12] C. M. Bellingham, K. A. Woodhouse, P. Robson, S. J. Rothstein, F. W. Keely, *Biochem. Biophys. Acta* **2001**, *1550*, 6.
[13] D. Kurkova, J. Kriz, P. Schmidt, J. Dybal, J. C. Rodriguez-Cabello, M. Alonso, *Biomacromolecules* **2003**, *4*, 589.
[14] B. Frohm, J. E. DeNizio, D. S. M. Lee, L. Gentile, U. Olsson, J. Malm, K. S. Akerfeldt, S. Linse, *Soft Matter* **2015**, *11*, 414.
[15] J. R. McDaniel, J. Bhattacharyya, K. B. Vargo, W. Hassouneh, D. A. Hammer, A. Chilkoti, *Angew. Chem. Int. Ed.* **2013**, *52*, 1683.
[16] I. González de Torre, L. Quintanilla, G. Pinedo-Martín, M. Alonso, J. C. Rodríguez-Cabello, *ACS Appl. Mater. Interfaces* **2014**, *6*, 14509.
[17] D. H. T. Le, R. Hanamura, D.-H. Pham, M. Kato, D. A. Tirrell, T. Okubo, A. Sugawara-Narutaki, *Biomacromolecules* **2013**, *14*, 1028.
[18] V. Aseyev, H. Tenhu, F. M. Winnik, *Adv. Polym. Sci.* **2011**, *242*, 29.
[19] M. Schönhoff, A. Larsson, P. B. Weizel, D. Kuckling, *J. Phys. Chem. B* **2002**, *106*, 7800.